OXFORD

Precision Clinical Medicine, 4(3), 2021, 168–175

https://doi.org/10.1093/pcmedi/pbab021
Advance Access Publication Date: 19 August 2021
Research Article

RESEARCH ARTICLE

CRISPR/Cas9 mediated somatic gene therapy for insertional mutations: the *vibrator* mouse model

Xin Fu[1,*,§], Jie Zhu[2,§], Yaou Duan[3,§], Paul Lu[4,5] and Kang Zhang[6,*]

[1]Spine Center, Xin Hua Hospital Affiliated to Shanghai Jiao Tong University School of Medicine, Shanghai 200092, China
[2]Guangzhou Women and Children's Medical Center, Guangzhou Medical University, Guangzhou 510623, China
[3]Department of Nanoengineering, Chemical Engineering Program, and Moores Cancer Center, University of California at San Diego, La Jolla, CA 92093, USA
[4]VA-San Diego Healthcare System, San Diego, CA 92161, USA
[5]Department of Neurosciences, University of California at San Diego, La Jolla, CA 92093, USA
[6]Center for Biomedicine and Innovations, Faculty of Medicine, Macau University of Science and Technology, Macao, China

*Correspondence: Xin Fu, fuxin032@yahoo.com; Kang Zhang, kang.zhang@gmail.com
§Xin Fu, Jie Zhu, and Yaou Duan contributed equally to this work.

Abstract

Somatic gene therapy remains technically challenging, especially in the central nervous system (CNS). Efficiency of gene delivery, efficacy in recipient cells, and proportion of cells required for overall benefit are the key points needed to be considered in any therapeutic approach. Recent efforts have demonstrated the efficacy of RNA-guided nucleases such as CRISPR/Cas9 in correcting point mutations or removing dominant mutations. Here we used viral delivered Cas9 plasmid and two guide RNAs to remove a recessive insertional mutation, *vibrator* (*vb*), in the mouse brain. The *vb* mice expressed ~20% of normal levels of phosphatidylinositol transfer protein, α (PITPα) RNA and protein due to an endogenous retrovirus inserted in intron 4, resulting in early-onset tremor, degeneration of brainstem and spinal cord neurons, and juvenile death. The *in situ* CRISPR/Cas9 viral treatment effectively delayed neurodegeneration, attenuated tremor, and bypassed juvenile death. Our studies demonstrate the potential of CRISPR/Cas9-mediated gene therapy for insertional mutations in the postnatal brain.

Key words: somatic gene editing; neurodegenerative disease; *vibrator* mouse model; CRISPR/Cas9; *Pitpna*

Introduction

The CRISPR/Cas system (clustered regularly interspaced short palindromic repeats/CRISPR-associated genes or proteins) is a defense mechanism found in bacteria which readily displays sequence specificity derived from Watson-Crick complementary base-pairing.[1,2] Since it permits site-specific modifications within complex genomes, it has been widely applied in both basic and clinical researches. CRISPR/Cas9 mediated gene therapy has shown promising results in treating many human

Received: 18 May 2021; **Revised:** 25 July 2021; **Accepted:** 11 August 2021

diseases, including cancers,[3,4] retinal diseases,[5,6] and Duchenne muscular dystrophy (DMD).[7–9] Despite its wide application in gene therapy, few studies have reported effective application of CRISPR-mediated gene therapy on neurodegenerative diseases, probably due to cell type complexity of the nervous system. In addition, the difficulty of promoting specific editing in sufficient numbers of target cells also obstacles application of gene therapy in neurodegenerative diseases.

In this study, we applied a gene editing strategy mediated by CRISPR/Cas9 to a neurodegenerative mouse model, *vibrator* (*vb*). The *vb* mutation is caused by the insertion of an endogenous retrovirus (intra-cisternal A particle; IAP) into the 4th intron of the *Pitpna* gene, which interferes with normal processing of nascent transcripts, resulting in ~5-fold loss of PITPα protein expression. Homozygous *vb* animals have severe neurological deficits, neurodegeneration in brainstem and spinal cord, which is reflected by severe action tremor and fully penetrant juvenile lethality.[10–12] Mice that completely lack PITPα were further detected to suffer from intestinal and hepatic steatosis and hypoglycemia.[13] A natural variant of *Nxf1* acts as a dose-dependent modifier of *vb* and other IAP insertions,[14–16] suggesting that *vb* would provide a useful phenotypic range to explore therapeutic potential of target removal of an insertional mutation.

Here we report the successful removal of the *vb* IAP using adenovirus associated virus (AAV) delivery of CRISPR/Cas9, correcting *Pitpna* expression in *vb* mouse brain and spinal cord. The somatic deletion of IAP sequences in recipient cells partially restored tissue-level PITPα expression. More importantly, the deletion of IAP effectively attenuated action tremor, delayed neurodegeneration, and improved the survival of *vb* mice. Our findings provide a promising postnatal approach that targets neurons in the central nervous system (CNS). CRISPR/Cas9 mediated gene therapy has vast potential. Our results suggest that remediation of insertional mutations using dual guide sequences is an advantageous approach for application, which pave the way for future exploration of CRISPR/Cas9 mediated gene therapy in other disorders.

Methods

Animals

Congenic C57BL/6J (B6)–*Pitpna*^{vb} mice (N43) were kind gifts from Bruce Hamilton's lab. The *Pitpna*^{vb} mice were maintained by backcross as described.[16] All mouse experiments were approved by the IACUC committee. All procedures were conducted with the approval and under the supervision of the Institutional Animal Care Committee at the University of California San Diego.

Plasmids

To construct dual gRNA expressing vectors, pAAV-U6 gRNA-EF1a GFP was used. Both 20 bp target sequences were constructed into the vector separately. Second gRNA together with U6 promoter was then amplified and inserted into the first gRNA expression vector. The CRISPR/Cas9 target sequences (20 bp target and 3 bp PAM sequence showed with underline) used in this study are shown as following: gRNA-L: GATACTCCTGTTTAGTGA TCGGG, gRNA-R: CTGGCCTGGTGTTATGACCCTGG. The pAAV-nEFCas9 (nEF, hybrid EF1α/HTLV) was previously published.[17]

AAV production

All AAVs were packaged with serotype 8 and were generated by the Gene Transfer Targeting and Therapeutics Core (GT3) at the Salk Institute for Biological Studies.

AAV injection in newborn mice

Genotyped newborn *vb* mice were randomly assigned to receive AAV injection or PBS treatment at postnatal day 2. The *vb* mice were anesthetized on ice, and 2 μl of AAV8 mixture (AAV-Cas9 (3×10^{10} GC) and AAV-gRNA L + R (3.6×10^{10} GC)) or 2 μl of PBS was injected through cerebellum and 3mm down into brainstem area using a 22s G syringe (Hamilton, #87 943). The needle was kept in site for 3 seconds before pulling out. The injection site was located by crossing a line between two ears and the extension of sagittal suture. For all injections, stereotaxic injection was used to control the location and depth of injection.

Tremor phenotype scoring

Tremor phenotype was scored based on an established method described previously.[15] Briefly, tremor phenotype was accessed by five independent investigators, blinded to genotypes, using a numerical scale of severity based on the distinctive behaviors. The mouse with the most severe tremor phenotype was given a highest score (5) and the mouse with no tremor was given a score of 0.

Histology

The *vb* mice were trans-cardially perfused with saline and then 4% paraformaldehyde. The whole brain with spinal cord was removed and left in PFA for 24 hours, dehydrated in 30% sucrose overnight, and embedded in OCT. Sagittal sections (15μm) were used for luxol fast blue-cresyl violet staining.

Immunofluorescence

Free floating whole brain and spinal cord sections (30 μm) were used for immunofluorescent staining. Brain and spinal cord sections were rinsed in TBS and blocked in 0.5% Triton X-100 in 5% BSA in PBS for 1 hour at room temperature, followed by an overnight incubation in primary antibodies at 4°C. After three washes in PBS, sections were incubated with secondary antibody. Cell nuclei were counterstained with DAPI (49,6-diamidino-2-phenylindole). The following antibodies were used:

chicken anti-GFP antibody (AVES, GFP-1020), mouse anti-HA antibody (Abcam, AB9110), and mouse anti-NeuN antibody (Millipore MAB377). The secondary antibodies, Alexa Fluor-488- or 555-conjugatedanti-mouse, rabbit, or chicken immunoglobulin G (IgG) (Invitrogen) were used at a dilution of 1:500. Sections were mounted with Fluoromount-G (Southern Biotech) and coverslipped. Images were captured using an Olympus FV1000 confocal microscope.

Fluorescence intensity quantification

Peak NeuN fluorescence intensity was quantified using ImageJ. The cross section of spinal cord was captured using Olympus FV1000 confocal microscope at 400X. Same exposure time was used for all images. Bright, relatively large, and in-focus cell perimeters were outlined freehand. An adjacent background area was selected for each cell. Corrected total cell fluorescence was calculated by subtracting the product of the area of a cell and the mean gray value of its respective background selection from the integrated density of the cell. A total of twenty cells from each zone (dorsal, intermediate, and ventral) were analyzed for each subject of wild type controls and treated vibrators, while all cells were analyzed for vibrator mutants.

DNA and RNA analyses of the mouse brain tissue

DNA or RNA was isolated from sagittal sectioned whole brain and spinal cord tissue using an FFPE DNA or RNA Mini Kit (Qiagen). DNA was further used for PCR and TOPO sequencing. PCR products were purified by gel extraction using QIAquick columns, and subsequently cloned into the pCR2.1-TOPO vector (Invitrogen). Eight clones from each sample were sequenced with the M13 universal primer. cDNA was synthesized from RNA using a Superscript III reverse transcriptase kit according to the manufacturer's instructions (Invitrogen). Quantitative PCR was performed via 40 cycle amplification using Power SYBR Green PCR Master Mix on a 7500 Real-Time PCR System (Applied Biosystems) with following primers: wt-F: TTGGGTACACAGCAAGACCA; IAP-F: AACGCGTCTAATAACACTTGTG; wt-rev: CCAAAAGGAC TGCCAGTCAT; *pitpna*-F-mRNA: ACACGAGAAAGCCTGG AATG; *pitpna*-R-mRNA: CACATGTTTCCATGCCTCAG; ga pdh-F-mRNA: CGTCCCGTAGACAAAATGGT; gapdh-R-m RNA: TTGATGGCAACAATCTCCAC. Measurements were performed in triplicate and normalized to endogenous GAPDH levels. The relative fold change in expression was calculated using the $\Delta\Delta$CT method (CT values < 30).

Rotarod test

The motor coordinating activity of the mouse was measured by its performance on a rotarod in the SDI ROTOR-ROD system (San Diego Instruments, San Diego, CA). The mouse was trained 3 times and rest for 30 min before subjected to the rotarod test. The rotating speed was set as accelerating gradually from 0 to 25 rpm, and the latency to fall from the rotating drum was recorded. The cut-off time for the latency to fall was 200 s. Mean latency from 3 tests was used for statistical analysis.

Statistics

Statistical software Graphpad Prism 7 was used for all statistical analyses. Data were analyzed using either *t*-test (mRNA and immunofluorescent staining), one-way ANOVA (tremor severity and rotarod test), or two-way ANOVA (NeuN immunofluorescent staining).

Results

To remove the intron 4 IAP sequences from the *Pitpna* gene, we generated a delivery system with two AAV vectors: one AAV vector expressing two gRNAs targeting sequences flanking IAP element, and the other expressing spCas9. As a result, the expression of PITPα could be restored after IAP element was cut from *Pitpna* gene (Fig. 1A and Sup. Fig. S1). Two gRNAs, flanking the IAP, with the highest score predicted by CRISPR design tool (http://www.rgenome.net/cas-designer/) were chosen (Fig. 1B) and constructed into an AAV vector. To test the editing efficiency, we co-transfected the two AAV vectors into *vb* mouse derived embryonic fibroblast (MEF) and assessed the removal or retention of the IAP by PCR. An assay for the wild-type allele, using two PCR primers flanking the IAP, showed a lower-molecular weight band only from genomic DNA in the group transfected with AAV vectors expressing two gRNAs and Cas9, but not in control groups, indicating CRISPR-dependent removal of IAP (Fig. 1C and D). Furthermore, we analyzed the potential off-target loci by blasting the gRNAs sequences in mouse genome, of which the majority of off-targets were located in intergenic and intronic region (Sup. Table S1).

We then separately packaged the dual-guide and Cas9 vectors into AAV serotype 8 (AAV8), which has shown optimal efficiency for infection of neurons in the brain.[18] A mix of two AAVs was injected into the brainstem area of newborn *vb* mice at postnatal day 2 ($n = 8$) after genotyping, in order to investigate the therapeutic efficacy of the *in situ* CRISPR/Cas9 viral treatment before juvenile death. Homozygous *vb* mice start to present action tremor at postnatal day 7–15, and juvenile lethality at postnatal day 15–30.[13] Presence of any tremor was videotaped and motor coordinating activity was recorded before the mice were sacrificed 30 days after AAV injection. Furthermore, motor coordinating activity was recorded in mice that were used for survival analysis until natural death. All *vb* mice ($n = 10$) showed progressive action tremor starting on Day 7 (Sup. Video 1). With AAV treatment, the onset of the tremor was significantly delayed and the severity of this symptom was dramatically attenuated (Sup. Video 2). Notably, 2 out of 10 *vb* mice lost mobility completely at a late stage, as well as developed hemiplegia and epileptic attacks (Sup. Video 3, Mice 3 and 4). However, their littermates with AAV treatment (2 out of 8 treated *vb* mice) showed

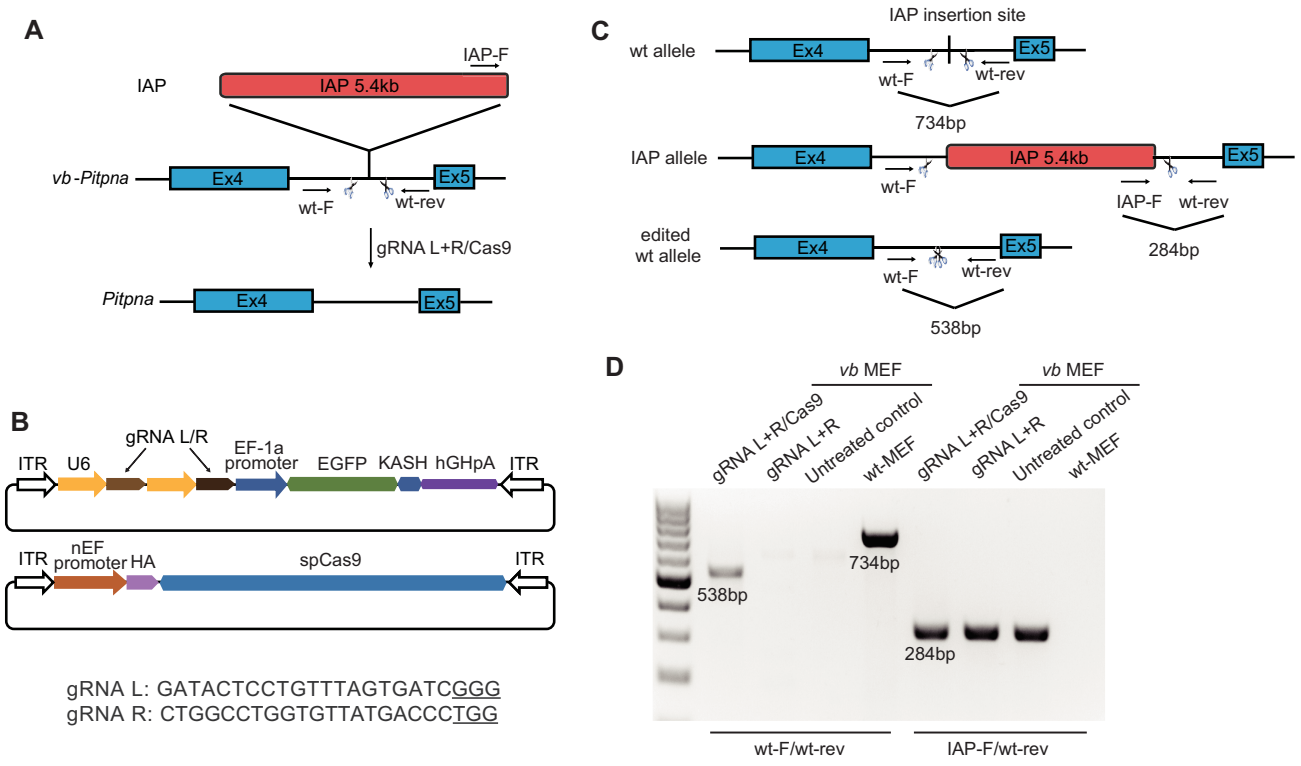

Figure 1. Design and validation in mouse embryonic fibroblasts (MEFs). **A**, Schematic of the *Pitpna*^{vb} *locus*. **B**, Schematic of the AAV vector design and target sequences for IAP element removal from *Pitpna* gene in *vb*. Locations of the guide RNA (gRNA) sequences to the left (L) and right (R) of the IAP are indicated by scissors. AAV vectors show inverted terminal repeats (ITR), U6 promoters for gRNA expression, and synthetic elements for EGFP expression to mark infected cells are indicated. PAM sequences are underlined. **C**, Primer design for verification of wild type, IAP insertion, and edited wild type allele. The primer sequences are indicated in method section. **D**, PCR assay to detect IAP element removal in *vb* MEFs. MEFs were co-transfected by CRISPR/spCas9 and gRNA vectors. PCR was carried out using genomic DNA. The sizes of PCR amplicons were indicated on the gel.

significantly improved mobility (Sup. Video 3, Mice 1 and 2). Tremor phenotype was accessed by five independent investigators, blinded to genotypes, using a numerical scale of severity based on the distinctive behaviors as descried previously.[15] The *vb* mice showing the most severe tremor phenotype were rescued by AAV treatment (Fig. 2A). Moreover, motor coordination was measured by examining the mice's performance on a rotarod on Day 25.[19] Untreated *vb* mice could barely stand on the rotor even after training, while AAV treated group showed a significantly increased latency (Fig. 2B). Taken together, AAV treatment attenuated symptoms of tremor and partially rescued the mobility of the *vb* mice. Survival rates of *vb* mice were also recorded. Over 50% of *vb* mice died within one week after birth and only 20% survived up to 30 days. In contrast, 80% of *vb* mice with AAV treatment (n = 8) bypassed juvenile lethality and reached a maximum survival of 40 days, indicating that local brainstem injection partially improved survival rate of *vb* mice (Fig. 2C).

We next evaluated the extent of IAP removal and recovery of *Pitpna* gene expression after the CRISPR/Cas9 AAV treatment. The infection of gRNA and spCas9 viruses was first confirmed by GFP and HA immunofluorescent staining respectively (Fig. 3A). Both GFP and HA expressions were observed in the cerebellum and brainstem regions, with approximately 12.5% GFP and HA co-staining efficiency, indicating successful transduction of these two viruses (Fig. 3A). IAP removal was analyzed at both DNA and RNA levels using brain tissues of injected mice. Similar to the result of *in vitro* co-transfection of *vb* MEF with these two AAV vectors, genotyping results showed successful removal of *Pitpna* IAP element in *vb* mouse brain (Fig. 3B). Sequencing results confirmed the sequence of the removed junction (Fig. 3C). More importantly, mRNA expression of *Pitpna* in brain tissue was rescued by 10% after AAV treatment (Fig. 3D). Together, these results demonstrated successful IAP removal and restored *Pitpna* expression in cells co-transduced by AAV vectors in *vb* mouse brain.

Reduced *Pitpna* expression results in a high degree of neuropathology in *vb* mice.[10–12] We therefore analyzed neurodegeneration in *vb* mice with or without AAV treatment. Morphological changes in neurons were first evaluated with luxol fast blue-cresyl violet (LFB-CV) staining. Significant morphological changes were observed in *vb* mice, including highly vacuolated cells, shrunken and pyknotic neurons, completely dark cells, and abnormally lightly stained cells without discrete intracellular

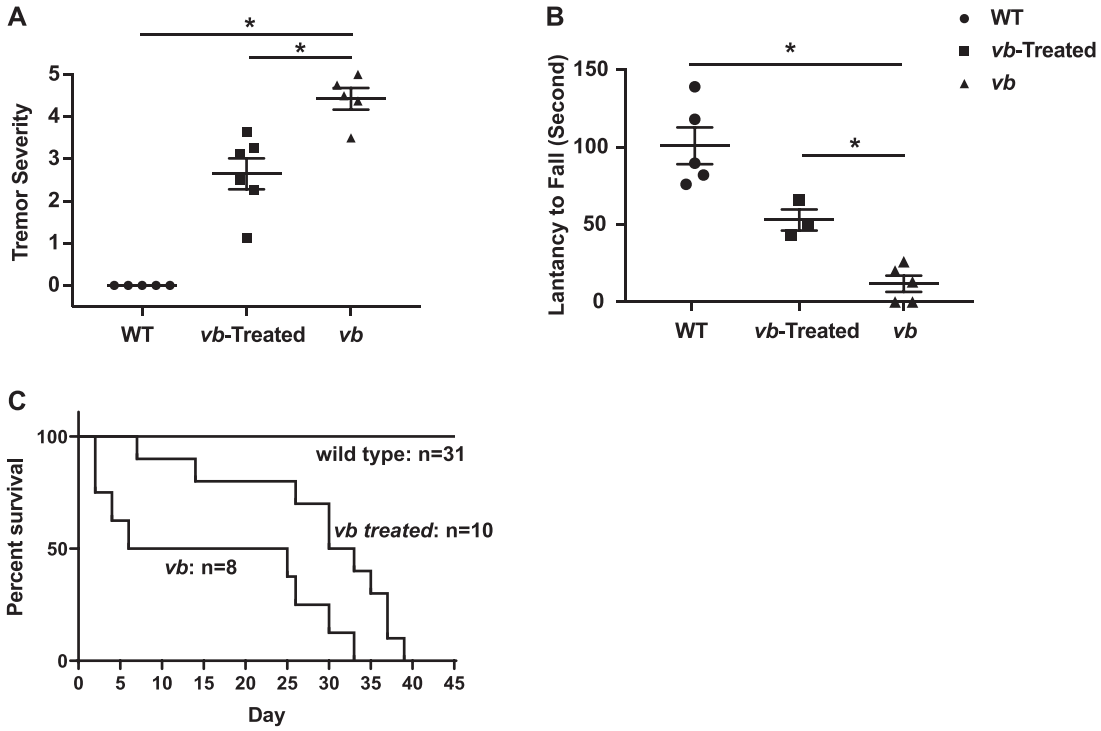

Figure 2. Improved tremor phenotype and motor coordination in treated vs. untreated animals. **A**, Improved tremor phenotype in AAV treated animals compared to untreated controls. Tremor phenotype was accessed by five independent investigators blind to genotype using a numerical scale of severity based on the distinctive behaviors. N = 5 for both wt and untreated *vb* groups. N = 6 for AAV treated *vb* group. **B**, Motor coordination was significantly improved in *vb* mice after AAV treatment. The test was performed around postnatal Day 25. Each mouse was trained 3 times and rested for 30 min before testing. The rotating speed accelerated gradually from 0 to 25 rpm, and the latency to fall from the rotating drum was recorded. Mean latency from 3 tests was used for statistical analysis (*$P < 0.05$; One-way ANOVA test; wild type and *vb*, n = 5; *vb* treated, n = 3). **C**, Survival curve of *vb* mice treated with CRISPR/Cas9 AAV. The life span of wild type, *vb*, and *vb* with AAV treatment was recorded. Total cohort sizes were indicated.

structure (Fig. 4A (arrows), B and Sup. Fig. S2). These features were barely observed in *vb* mice after AAV treatment; statistical analysis showed a significant reduction of vacuolated cells in the AAV treated group as compared to the untreated group (Fig. 4A, B and Sup. Fig. S2). Besides neuropathology in the region of brainstem, dramatic neuronal change in spinal cord region was also observed. Immunofluorescent staining of neuronal marker NeuN (*Rbfox3*, RNA binding protein, fox-1 homolog 3) and motor neuron marker ChAT (choline acetyltransferase) showed dramatic differences on the upper lumbar region of the spinal cord (Lumbar level 2 to 3) among wild type and *vb* mice, including the intensity of NeuN labeling, the size of $NeuN^+$ cells, as well as the numbers and sizes of $ChAT^+$ motor neurons (Fig. 4C–G). These features indicated neurodegeneration in the region of spinal cord in *vb* mice. After AAV treatment, we observed a partial restoration in fluorescence intensity and cell sizes labeled by NeuN at dorsal, intermediate, and ventral zones (Fig. 4D and E). The number and size of motor neurons, labelled by ChAT, was also increased in *vb* mice treated with AAV vectors compared to untreated controls (Fig. 4F and G). Taken together, CRISPR/Cas9 AAV treatment reduced neuronal degeneration in *vb* mice, especially in ChAT positive motor neurons.

Discussion

The development of therapeutic strategies for CNS disorders is challenging, given the complexity of cells and neural circuits involved, poor tissue regeneration ability, and incomplete understanding of pathological processes. The treatment method, typically the timing of treatment, drug-delivery mechanism, drug dose, drug-related toxicity, needs systemic investigation. In this study, we showed that CRISPR/Cas9 effectively removed an IAP endogenous retrovirus from *Pitpna* gene in *vb* mouse brain and spinal cord by a single dose of AAV injection in the region of brain at neonatal stage. The effect of this gene editing treatment is dramatic; it reduced neurodegeneration, attenuated action tremor, and extended lifespan of *vb* mice. This finding suggests that there is a great potential in the CRISPR/Cas9 mediated gene therapy to treat CNS disorders.

Although the therapeutic efficacy of CRISPR/Cas9 mediated gene therapy is profound, this first-generation somatic treatment did not fully rescue *vibrator* phenotypes in this study. Two major reasons we proposed are (i) neural degeneration initiated at embryonic stage and our treatment timing was not early enough, and (ii) virus transduction efficiency was not high enough to fully reverse the neurodegeneration process. The second

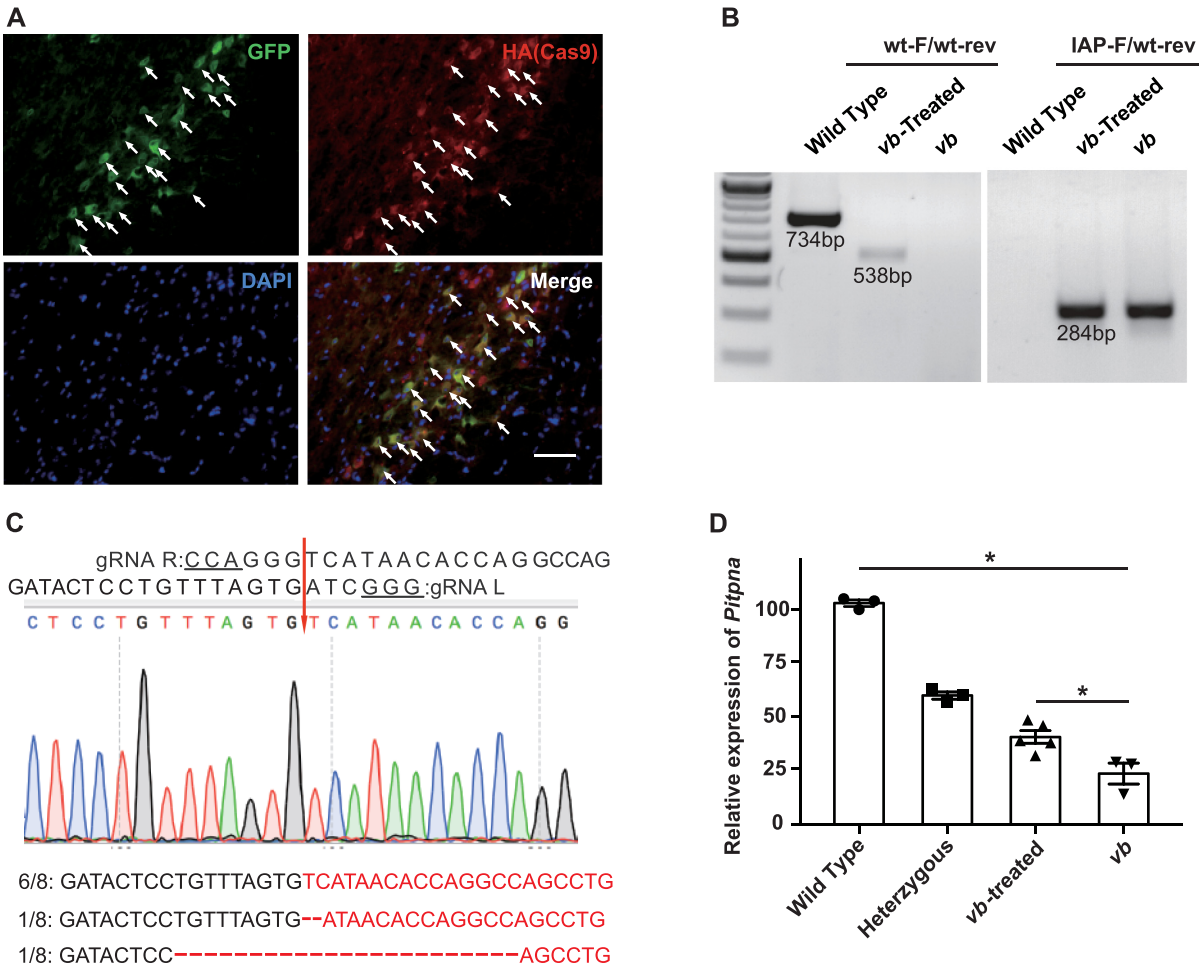

Figure 3. CRISPR/spCas9 AAV-treatment removed the *Pitpna* IAP element in *vb* mice brain. **A**, Immunofluorescent analysis of GFP and HA tag in injected *vb* mice brain treated with AAV-gRNA L + R-GFP and AAV-Cas9-HA. The *vb* mice were treated at postnatal day 2 (P2) and harvested at P30. Sagittal section of central brain tissue close to dorsal Pons area was used for immunofluorescent staining. Arrows indicate cells infected by AAV-gRNA L + R-GFP and AAV-Cas9-HA vectors. GFP, green; HA, Red; DAPI, blue. Scale bar: 50 μm. **B**, IAP element cutting from *Pitpna* gene in *vb* mice brain. 8–10 sagittal sections (10 μm) of central brain tissue with partial spinal cord were used for genomic DNA extraction and wt/IAP amplification. The sizes of PCR amplicons were indicated on the gel. **C**, Genomic DNA from panel B was amplified and cloned into pCR2.1-TOPO vector and 8 single colonies were sequenced. Most (6/8) showed precise joining at the predicted cut sites for the two guide RNAs; two singleton clones showed deletion of 2 or 23 additional bases. **D**, RT-qPCR analysis of *Pitpna* mRNA expression. 8–10 sagittal sections (10 μm) of central brain tissue with partial spinal cord were used for total RNA extraction and RT-qPCR. The expression level of *Pitpna* for one animal was averaged by 3 groups of brain sections, and at least 3 mice of each group were used for statistical analysis ($P = 0.018$. Student's *t*-test, $n \geq 3$).

reason raises another critical issue for AAV related gene therapy in the field for future investigation: how to define a drug dose with both high tissue transduction and tolerated toxicity. Moreover, efficiency of virus transduction is not equal across different zones of brain and spinal cord. In this study, we observed higher transduction efficiency in the brainstem zone (Fig. 3A) and the dorsal area of spinal cord (Fig. 4C), as well as in the ChAT$^+$ motor neurons (Fig. 4C) than other regions.

Recently, researchers have explored gene therapies on many neurodegenerative disorders. For instance, Yang *et al.* used a CRISPR/Cas9 strategy to edit a dominant mHTT (mutant huntingtin) gene in the striatum in mHTT-expression mice, which showed an attenuated neuropathology.[20] CRISPR/Cas9 nanocomplexes was also used to target Bace1 suppressed amyloid beta (Aβ)-associated pathologies and cognitive deficits in two mouse models of Alzheimer's disease.[21] Moreover, genome editing of SOD1 mediated by AAV9-CRISPR/Cas9 resulted in improved motor function and reduced muscle atrophy in SOD1 G93A amyotrophic lateral sclerosis (ALS) mouse model.[22] These findings demonstrate an increasingly promising future for gene therapy in CNS.

In our study, we showed targeted genomic editing for a recessive disorder in a different CNS compartment with notable improvement on several phenotypes. This finding suggests that there is a great potential in the CRISPR/Cas9 mediated gene therapy to treat insertional or expansion mutations. More importantly, the treatment is independent of the disease inheritance model. Our approach demonstrates that CRISPR/Cas9 mediated gene editing could be a novel approach to treat neuronal disease by somatically targeting germline mutations in the CNS to remove damaging sequences.

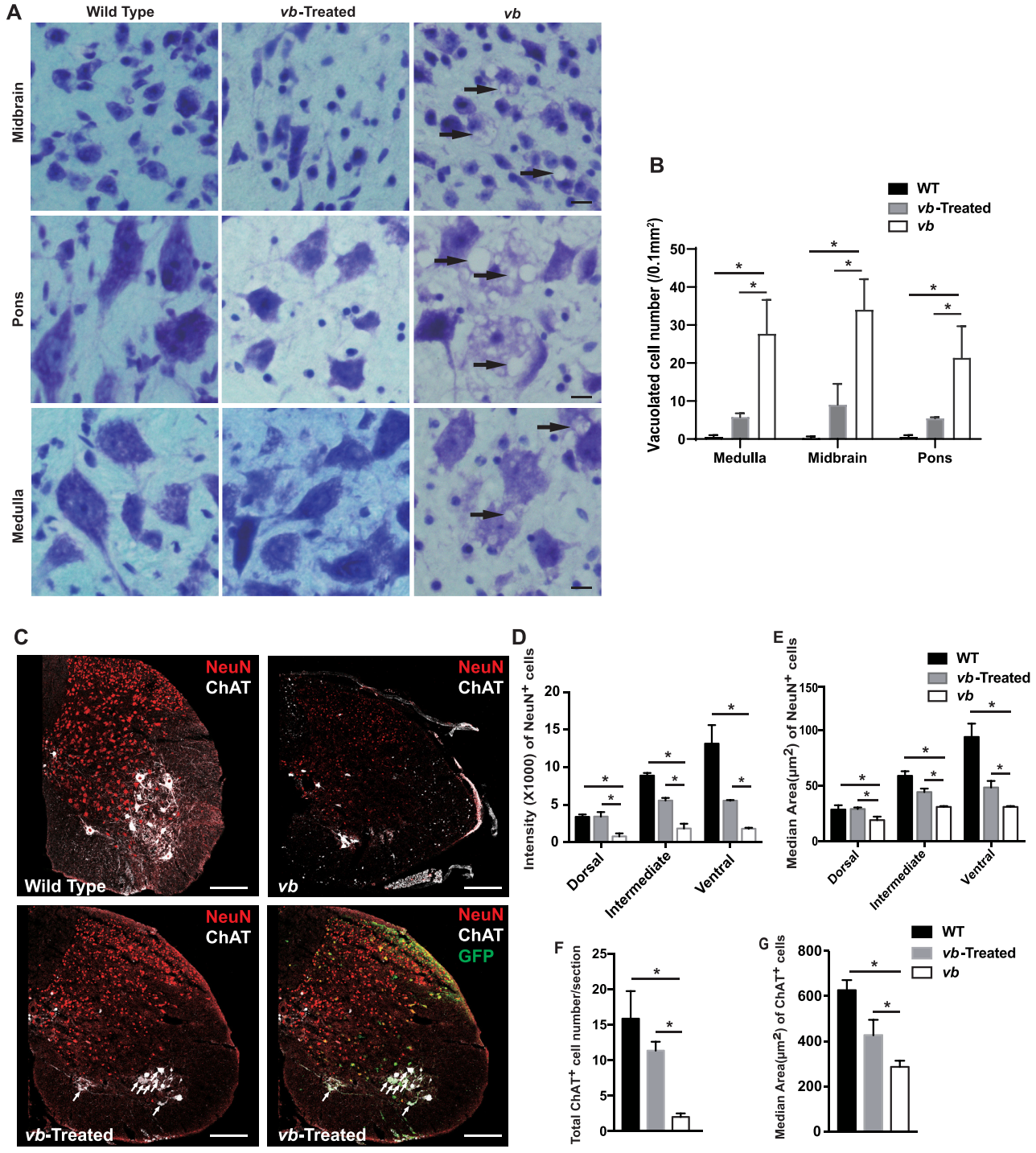

Figure 4. CRISPR/spCas9 AAV-treated *vb* mice had less neuronal degeneration. **A**, Luxol fast blue-cresyl violet staining of brain tissue (midbrain, pons, and medulla area) treated with AAV-gRNA L + R-GFP and AAV-Cas9-HA. Scale bar, 10μm. Arrows indicated vacuolated cells observed in the region of brainstem in *vb* mice. **B**, quantification of vacuolated cell numbers in Panel A. At least 5 pictures were randomly chosen and total vacuolated cell numbers per 0.1 mm^2 were calculated for each mouse. Results are shown as mean ± s.e.m. (*$P < 0.05$. 2-way ANOVA, n = 4 for wt and *vb* treated, n = 3 for *vb* mutant). **C**, Immunofluorescent analysis of NeuN and ChAT in *vb* spinal cord treated with AAV-gRNA L + R-GFP and AAV-Cas9- HA. Cross sections of lumbar spinal cord were used. NeuN, red; ChAT, grey; GFP, green; DAPI, blue. Scale bar: 200μm. Arrows indicate GFP and ChAT double positive motor neurons in *vb* treated mice. **D**, quantification of $NeuN^+$ cell fluorescence intensity in Panel C. **E**, quantification of cell area of $NeuN^+$ cells. $NeuN^+$ cells were grouped into dorsal, intermediate, and ventral zone. Totally 50 cells at each zone were randomly chosen and median area was calculated for each mouse. Results are shown as mean ± s.e.m. (*$P < 0.05$. 2-way ANOVA, n = 4 for wt and *vb* treated, n = 3 for *vb* mutant). **F-G**, quantification of cell number (F) and area (G) of $ChAT^+$ cells in Panel C. Median area were calculated by all $ChAT^+$ cells for each mouse, and results are shown as mean ± s.e.m. (*$P < 0.05$. ANOVA test, n = 4 for wt and *vb* treated, n = 3 for *vb* mutant).

Supplementary data

Supplementary data is available at PCMEDI online.

Author contributions

X.F., J.Z., Y.D., and P.L. performed mouse *in-vivo* experiments and functional analysis. X.F. and Y.D. performed gene editing work. X.F., J.Z., and Y.D. analyzed data. X.F. and K.Z designed the study and wrote the paper. All authors discussed the results and commented on the manuscript.

Acknowledgements

This research was funded by the National Natural Science Foundation of China (grant No. 3201101229), Macao Science and Technology Development Fund(grant No. 015/2017/AFJ), and Natural Science Foundation of Guangdong Province (grant No. 2020A1515010072).

Conflict of interest

The authors declare no competing financial interests. Besides, as a Co-EIC of *Precision Clinical Medicine*, the corresponding author Dr. Kang Zhang was blinded from reviewing or making decisions on this manuscript.

References

1. Doudna JA, Charpentier E. Genome editing. The new frontier of genome engineering with CRISPR-Cas9. *Science* 2014;**346**:1258096. doi:10.1126/science.1258096.
2. Hsu PD, Lander ES, Zhang F. Development and applications of CRISPR-Cas9 for genome engineering. *Cell* 2014;**157**:1262–78. doi:10.1016/j.cell.2014.05.010.
3. Ren J, Liu X, Fang C, *et al*. Multiplex genome editing to generate universal CAR T cells resistant to PD1 inhibition. *Clin Cancer Res* 2017;**23**:2255–66. doi:10.1158/1078-0432.CCR-16-130. 0
4. Cyranoski D. Chinese scientists to pioneer first human CRISPR trial. *Nature* 2016;**535**:476–7. doi:10.1038/nature.2016.20302.
5. Yu W, Mookherjee S, Chaitankar V, *et al*. Nrl knockdown by AAV-delivered CRISPR/Cas9 prevents retinal degeneration in mice. *Nat Commun* 2017;**8**:14716. doi:10.1038/ncomms14716.
6. Zhu J, Ming C, Fu X, *et al*. Gene and mutation independent therapy via CRISPR-Cas9 mediated cellular reprogramming in rod photoreceptors. *Cell Res* 2017;**27**:830–3. doi:10.1038/cr.2017.57.
7. Long C, Amoasii L, Mireault AA, *et al*. Postnatal genome editing partially restores dystrophin expression in a mouse model of muscular dystrophy. *Science* 2016;**351**:400–3. doi:10.1126/science.aad5725.
8. Nelson CE, Hakim CH, Ousterout DG, *et al*. In vivo genome editing improves muscle function in a mouse model of Duchenne muscular dystrophy. *Science* 2016;**351**:403–7. doi:10.1126/science.aad5143.
9. Tabebordbar M, Zhu K, Cheng JK, *et al*. In vivo gene editing in dystrophic mouse muscle and muscle stem cells. *Science* 2016;**351**:407–11. doi:10.1126/science.aad5177.
10. Concepcion D, Johannes F, Lo YH, *et al*. Modifier genes for mouse phosphatidylinositol transfer protein alpha (vibrator) that bypass juvenile lethality. *Genetics* 2011;**187**:1185–91. doi:10.1534/genetics.110.125906.
11. Hamilton BA, Smith DJ, Mueller KL, *et al*. The vibrator mutation causes neurodegeneration via reduced expression of PITP alpha: positional complementation cloning and extragenic suppression. *Neuron* 1997;**18**:711–22. doi:10.1016/S0896-6273(00)80312-8.
12. Weimar WR, Lane PW, Sidman RL. Vibrator (vb): a spinocerebellar system degeneration with autosomal recessive inheritance in mice. *Brain Res*. 1982;**251**:357–64. doi:10.1016/0006-8993(82)90754-5.
13. Alb JG, Jr., Cortese JD, Phillips SE, *et al*. Mice lacking phosphatidylinositol transfer protein-alpha exhibit spinocerebellar degeneration, intestinal and hepatic steatosis, and hypoglycemia. *J Biol Chem* 2003;**278**:33501–18. doi:10.1074/jbc.M303591200.
14. Concepcion D, Ross KD, Hutt KR, *et al*. Nxf1 natural variant E610G is a semi-dominant suppressor of IAP-induced RNA processing defects. *PLos Genet* 2015;**11**:e1005123. doi:10.1371/journal.pgen.1005123.
15. Floyd JA, Gold DA, Concepcion D, *et al*. A natural allele of Nxf1 suppresses retrovirus insertional mutations. *Nat Genet-Nat Genet* 2003;**35**:221–8. doi:10.1038/ng1247.
16. Concepcion D, Flores-Garcia L, Hamilton BA. Multipotent genetic suppression of retrotransposon-induced mutations by Nxf1 through fine-tuning of alternative splicing. *PLoS Genet* 2009;**5**:e1000484. doi:10.1371/journal.pgen.1000484.
17. Suzuki K, Tsunekawa Y, Hernandez-Benitez R, *et al*. In vivo genome editing via CRISPR/Cas9 mediated homology-independent targeted integration. *Nature* 2016;**540**:144–9. doi:10.1038/nature20565.
18. Broekman ML, Comer LA, Hyman BT, *et al*. Adeno-associated virus vectors serotyped with AAV8 capsid are more efficient than AAV-1 or -2 serotypes for widespread gene delivery to the neonatal mouse brain. *Neuroscience* 2006;**138**:501–10. doi:10.1016/j.neuroscience.2005.11.057.
19. Jones BJ, Roberts DJ. The quantiative measurement of motor inco-ordination in naive mice using an acelerating rotarod. *J Pharm Pharmacol* 1968;**20**:302–4. doi:10.1111/j.2042-7158.1968.tb09743.x.
20. Yang S, Chang R, Yang H, *et al*. CRISPR/Cas9-mediated gene editing ameliorates neurotoxicity in mouse model of Huntington's disease. *J Clin Invest* 2017;**127**:2719–24. doi:10.1172/JCI92087.
21. Park H, Oh J, Shim G, *et al*. In vivo neuronal gene editing via CRISPR-Cas9 amphiphilic nanocomplexes alleviates deficits in mouse models of Alzheimer's disease. *Nat Neurosci* 2019;**22**:524–8. doi:10.1038/s41593-019-0352-0.
22. Gaj T, Ojala DS, Ekman FK, *et al*. In vivo genome editing improves motor function and extends survival in a mouse model of ALS. *Sci AdvSci Adv* 2017;**3**:eaar3952. doi:10.1126/sciadv.aar3952.